# Surface-directed spinodal decomposition: Hydrodynamic effects

Hao Chen and Amitabha Chakrabarti
*Department of Physics, Kansas State University, Manhattan, Kansas 66506*
(Received 5 August 1996)

We present results from a numerical study of surface-directed spinodal decomposition in a binary fluid mixture, for critical and various off-critical concentrations. We explicitly add a long-range surface interaction term to the bulk free-energy functional leading to preferential attraction of one of the components of the fluid mixture to a solid surface. We also consider hydrodynamic interactions in these model calculations. Results of the wetting layer thickness and the domain size as a function of time and the scaling behavior of the density profile perpendicular to the surface are presented in the fluid inertia controlled regime. [S1063-651X(97)00105-0]

PACS number(s): 36.20.−r, 82.70.−y, 87.15.−v

## I. INTRODUCTION

Domain growth in a quenched binary fluid mixture is controlled by a variety of transport mechanisms due to the coupling of the order parameter to hydrodynamics [1,2]. It is well known that after an initial transient, the characteristic size of the domains, $R(t)$ grows with a power law $R(t) \sim t^n$, where $n$ is the domain growth exponent. The value of $n$ depends on the mechanism controlling the growth of domains. If the fluid mixture is of critical concentration, domain growth at *early times* is governed by a diffusive mechanism theoretically identified by Lifshitz and Slyozov [3]. This mechanism leads to the following growth law:

$$R(t) \sim t^{1/3}. \tag{1}$$

At late times, hydrodynamic effects become important and the growth exponent changes from the Lifshitz-Slyozov value of $n = \frac{1}{3}$. Depending on whether viscous forces or inertial effects of the critical fluid mixture dominate, the growth law can take one of the following forms [4–6]:

$$R(t) \sim t \quad \text{(viscosity controlled)}, \tag{2}$$

$$R(t) \sim t^{2/3} \quad \text{(fluid inertia controlled)}. \tag{3}$$

This dynamical behavior of phase separating fluids in the bulk is strongly affected by the presence of a wetting surface. The presence of a surface breaks the rotational and translational symmetry present in the isotropic bulk systems and affects domain formation. Due to the preferential attraction of one of the components (say the component $A$ of a generic $A-B$ mixture) to the surface, a wetting layer is formed on the attractive surface and the thickness of this wetting layer $l(t)$ grows with time $t$ with a power law [7]:

$$l(t) \sim t^{\theta}. \tag{4}$$

The corresponding density profile for the growing layer shows a damped oscillatory form as a function of the distance perpendicular to the surface. This so-called ''surface directed'' spinodal decomposition has been observed in various experiments [8–11] and in numerical simulations [7,12–16].

For diffusive growth and unstable bulk system, the growth of the wetting layer is similar to the bulk domain growth. Recent numerical simulations [12–15] and scaling analysis [7] suggest that the thickness of the wetting layer $l(t)$ grows with time as $t^{1/3}$ in the absence of hydrodynamic effects. Actually, Lifshitz and Slyozov [3] in their classic paper have already pointed this out in the context of crust sintering. Experimental studies of surface-directed spinodal decomposition in various polymer blends have confirmed the $t^{1/3}$ growth law for the wetting layer [9–11]. In these polymer blends hydrodynamic effects set in at a very late time due to the high viscosity of the blend, and the diffusive growth of the wetting layer is accessible over experimental time scales. Moreover, these experiments have also confirmed the dynamical scaling behavior for the density profile perpendicular to the wetting surface, first suggested by Brown and Chakrabarti [13] in a numerical study.

One expects that the inclusion of hydrodynamics would accelerate the growth of the wetting layer in a critical fluid mixture similar to its effects on bulk domain growth. A recent scaling analysis by Marko [7] has suggested that the growth of the wetting layer is characterized by the same growth exponent as the bulk domains. Some experiments [17] however, have shown the presence of a ''fast mode'' parallel to the surface. A theoretical explanation for the presence of this fast mode has been provided [18] in terms of anisotropically growing domains near the surface. But a detailed understanding of how hydrodynamics affect wetting layer growth is still lacking. This motivates us to perform a numerical study in a realistic model system. As a first step toward this goal, we consider a two-dimensional system, and numerically study the dynamics of phase separation of a binary fluid mixture of either critical or off-critical concentration, in the presence of a preferentially attractive surface. Although the two-dimensional results may not be applicable for a detailed understanding of experimental results of wetting layer growth, we expect that such a simulation would provide some insight into the role played by hydrodynamics on the wetting layer growth for various concentrations of the fluid mixture. It is important to note that for two-dimensional critical fluid mixtures, the growth laws in the presence of hydrodynamics are different from the three-dimensional ones listed in Eqs. (2) and (3), and are given by [5,6,19–22]

 

$$R(t)\sim t^{1/2} \quad \text{(viscosity controlled)}, \tag{5}$$

$$R(t)\sim t^{2/3} \quad \text{(fluid inertia controlled)}. \tag{6}$$

These theoretical results have recently been confirmed in large-scale two-dimensional simulations [21]. Moreover, simulations [22] also point out that for an off-critical fluid-mixture (75%-25% *composition*) in two dimensions the growth-exponent is given by $n\approx 0.46$.

In our simulations, we start from a Ginzburg-Landau expression for the free-energy functional of the bulk fluid mixture and explicitly add a long-range surface interaction term to mimic the van der Waals interactions that lead to the preferential attraction of one of the components of the mixtures to the free surface. The inclusion of hydrodynamics is modeled by introducing a coupling of the order parameter to a velocity field in the similar fashion as in the ''model H'' of Hohenberg and Halperin [1,24]. Domain growth in a bulk system characterized by this model H has been studied recently in both two and three dimensions. However, most of the previous simulations in model H are performed for *compressible* bulk fluid mixture [20–23] that simplifies the numerical calculation greatly. In contrast, we have strictly implemented the incompressibility condition in our simulations by introducing a streaming function and a vorticity function [25–27]. For our choice of the parameters of the model, domain growth at late times is controlled by fluid inertia. We provide the details of the model and the numerical calculations in Sec. II. In Sec. III we present our results for the morphology, growth exponent, and dynamical scaling behavior of the growing wetting layer for critical and several off-critical compositions of the fluid mixture. Finally, in Sec. IV, we conclude the paper with a brief summary and discussion of the results.

## II. MODEL AND NUMERICAL PROCEDURE

We start with a coarse-grained description of the ordering process in binary fluids. The main ingredient in this model is a conserved order parameter representing the local concentration difference coupled to one current. Renormalization-group arguments [6] suggest that such a model-*H* formulation, originally proposed for studying critical dynamics of a binary liquid mixture, should also be applicable for studying kinetics of domain growth in a quenched binary liquid. Recently, the applicability of this so-called model *H* [1] in the context of phase separation in binary fluid mixture has been discussed in detail by Jasnow and Vinals [24]. The presence of an interacting surface is included in the model by adding a long-range surface-interaction potential $V(y)\phi$ to the standard Ginzburg-Landau free-energy functional $F_{\rm bulk}$ used for the bulk free-energy. After a suitable rescaling of the order parameter, velocity, time, and space, the basic equations describing the dynamical evolution after quench can be written as [1,20,24,25]

$$\partial_t \vec{v} + g(\vec{v}\cdot\vec{\nabla})\vec{v} = \eta\nabla^2\vec{v} + g\mu\vec{\nabla}\phi, \tag{7}$$

$$\partial_t \phi = -g\vec{v}\cdot\vec{\nabla}\phi + \nabla^2\mu, \tag{8}$$

$$\vec{\nabla}\cdot\vec{v} = 0, \tag{9}$$

where $\phi$ is the order parameter $\vec{v}$ [$\equiv(u,v)$ in two dimensions] is the fluid velocity, $g$ is the coupling strength between the order-parameter and the hydrodynamic interactions, $\eta$ is the shear viscosity of the fluid, and $\mu$ is the rescaled local chemical potential [$\mu\equiv\delta F_{\rm bulk}/\delta\phi + V(y)$], which has the following form [13]:

$$\mu = \frac{\delta F}{\delta\phi} = -\phi + \phi^3 - \nabla^2\phi + V(y). \tag{10}$$

Equation (9) is the requirement of local incompressibility of the fluid that was neglected in some previous simulations of bulk fluid system [20–23].

We consider a $L_x\times L_y$ lattice with $L_x = L_y = 128$. The preferentially attracting surface is located at $y=0$. The specific form considered for the interaction potential is

$$V(y) = -\frac{\sigma}{y^{p+1}} \quad (y>0), \tag{11}$$

$$V(y) = -\sigma \quad (y=0), \tag{12}$$

where we have considered $\sigma = 0.4$ and $p=1$ and 2 in our simulations [13,15]. The boundary conditions in this study correspond to periodic boundary conditions in the $x$ direction and rigid-wall boundary conditions for the surfaces located at $y=0$ and $y=127$. These imply that

$$\frac{\partial\mu}{\partial y} = 0, \quad \frac{\partial\phi}{\partial y} = 0, \tag{13}$$

$$\vec{v} = 0 \tag{14}$$

at $y=0$ and $y=127$. Equation (13) is the requirement that no flux is allowed to go through the surfaces. Equation (14) is the no-slip boundary condition.

In two dimensions, one introduces the vorticity $\xi$ and the streaming function $\psi$ according to the following definitions [26]:

$$\xi = \frac{\partial u}{\partial y} - \frac{\partial v}{\partial x}, \tag{15}$$

$$u = \frac{\partial\psi}{\partial y}, \quad v = -\frac{\partial\psi}{\partial x}. \tag{16}$$

The basic equations then can be rewritten in the following numerically convenient forms [26–28]:

$$\frac{\partial\xi}{\partial t} + g\left[\frac{\partial(\xi u)}{\partial x} + \frac{\partial(\xi v)}{\partial y}\right] = \frac{\partial^2\xi}{\partial x^2} + \frac{\partial^2\xi}{\partial y^2} + g\left(\frac{\partial\phi}{\partial x}\frac{\partial\mu}{\partial y} - \frac{\partial\phi}{\partial y}\frac{\partial\mu}{\partial x}\right), \tag{17}$$

$$\nabla^2\psi = \xi, \tag{18}$$

$$\frac{\partial\phi}{\partial t} = -g\left[\frac{\partial(\phi u)}{\partial x} - \frac{\partial(\phi v)}{\partial y}\right] + \left(\frac{\partial^2\mu}{\partial x^2} + \frac{\partial^2\mu}{\partial y^2}\right). \tag{19}$$

The no-slip boundary condition [Eq. (14)] then implies

$$\psi=0, \quad \frac{\partial\psi}{\partial y}=0. \tag{20}$$

Under these boundary conditions, both the order parameter and vorticity remain as conserved quantities.

In the finite difference approximation of the partial differential equations (17), (18), and (19), the following definitions are employed:

$$x_j=j\Delta x, \quad y_k=k\Delta y, \quad t_n=n\Delta t, \tag{21}$$

$$Q_n=Q_n(j,k)=Q_n(x_j,y_k,t_n), \tag{22}$$

$$\nabla_x Q_n=[Q_n(j+1,k)-Q_n(j,k)]/\Delta x, \tag{23}$$

$$\nabla_x^2 Q_n=[Q_n(j+1,k)+Q_n(j-1,k)-2Q_n(j,k)]/(\Delta x)^2, \tag{24}$$

$$\mathcal{L}_x Q_n=[\nabla_x^2 Q_n-g\nabla_x(uQ_n)_n], \tag{25}$$

$$\mathcal{L}_y Q_n=[\nabla_y^2 Q_n-g\nabla_y(vQ_n)n]. \tag{26}$$

The operators $\nabla_y$ and $\nabla_y^2$ are defined in a similar way.

We use an alternating direction implicit method [27,29] to solve the parabolic equation (17), which can be written as

$$\frac{\partial\xi}{\partial t}=\mathcal{L}_x\xi+\mathcal{L}_y\xi+\varphi, \tag{27}$$

where

$$\varphi=g\left(\frac{\partial\phi}{\partial x}\frac{\partial\mu}{\partial y}-\frac{\partial\phi}{\partial y}\frac{\partial\mu}{\partial x}\right). \tag{28}$$

We write the above equation implicitly into two half steps,

$$\frac{\xi_{j,l}^{n+1/2}-\xi_{j,l}^{n}}{\Delta t/2}=\mathcal{L}_x\xi_{j,l}^{n+1/2}+\mathcal{L}_y\xi_{j,l}^{n}+\varphi^n, \tag{29}$$

$$\frac{\xi_{j,l}^{n+1}-\xi_{j,l}^{n+1/2}}{\Delta t/2}=\mathcal{L}_x\xi_{j,l}^{n+1/2}+\mathcal{L}_y\xi_{j,l}^{n+1}+\varphi^n. \tag{30}$$

These equations can be solved by a standard tridiagonal matrix-solving algorithm. Given $\xi^n$, we solve Eq. (29) for $\xi^{n+1/2}$, substitute $\xi^{n+1/2}$ into Eq. (30), and then solve $\xi^{n+1}$. The elliptic equation (18) is solved by using the successive over relaxation method with a Chebychev acceleration [29]

$$\psi_{j,l}^{n+1}=\psi_{j,l}^{n}+\omega\frac{\zeta_{j,l}}{4}, \tag{31}$$

where

$$\zeta_{j,l}=\psi_{j+1,l}+\psi_{j-1,l}+\psi_{j,l+1}+\psi_{j,l-1}-4\psi_{j,l}-\xi_{j,l}. \tag{32}$$

We adopt an odd-even ordering in processing the lattice points: we carry out one-half sweep updating the odd points, and then another half-sweep updating the even points with the new odd values. $\omega$ in Eq. (31) is the relaxation parameter that is changed at each half-sweep [29].

Equation (19) is solved straightforwardly by the Euler method. In our simulations, we use a time step of $\Delta t=0.01$ or 0.02, and mesh sizes $\Delta x=\Delta y=1$. We do not consider the effects of thermal noise terms in the evolution equations. This approximation is reasonable for deep quenches as there is some evidence that the noise term does not play an important role in the late stages of domain growth [6]. We write $\langle\phi\rangle=\phi_0=2x_0-1$, where the angular bracket denotes spatial average, and consider various values of $x_0$, the volume fraction of the component preferentially attracted to the surface. We also maintain $\langle\xi\rangle=0$ throughout the course of the simulations. Since we have not incorporated thermal noise in the simulation, some amount of randomness is needed in the initial distribution of the order parameter in order to allow for growth of the initial random nuclei. The initial values of $\phi$ are chosen randomly between $(\phi_0-0.1)$ and $(\phi_0+0.1)$, and the initial values of $\xi$ in the inner lattice points are chosen randomly between $-0.1$ and 0.1. At later times, the small inhomogeneities in the order parameter evolve into macroscopic domains of one or the other phase. The effect of hydrodynamics can be ''turned off'' (with a coupling constant $g=0$) or ''on'' $(g=1)$ conveniently in the simulations. For the diffusive case $(g=0)$ we only need to solve Eq. (19). For $g=1$, we need to solve the coupled equations. Given initial $\phi$ and inner $\xi$, Eq. (18) is used to get the corresponding $\psi$ field and then also used to figure out the vorticity values at the surfaces. The components of the velocity field, $u$ and $v$ are then calculated from $\psi$ and the results are used to advance $\phi$ and inner $\xi$ to the new time.

We compute the density profile as a function of distance from the wetting surface. This is defined as

$$n(y,t)=\frac{1}{L_x}\sum_{i=1}^{L_x}\psi(\vec{r}=(i,y),t). \tag{33}$$

The wetting layer thickness is obtained from the density profile as the smallest value that satisfies

$$n(l(t),t)=\phi_0. \tag{34}$$

The bulk domain sizes are obtained by computing the pair-correlation function $g_x$ and $g_y$ along and perpendicular to the surface. The pair-correlation function $g_y$, for example, is defined as

$$g_y(y,t)=\frac{1}{L_x}\sum_{i=1}^{L_x}g_{y_t}(y,t), \tag{35}$$

where $g_{y_i}$ is defined as

$$g_{y_i}(y,t)=\left\langle\sum_j\phi(\vec{r}=(i,y),t)\phi(\vec{r}=(i,j+y),t)-\phi_0^2\right\rangle. \tag{36}$$

A similar expression can be written for the pair-correlation function $g_x$. The locations of the first zeros of these functions are taken as measures of average domain sizes $R_x(t)$ and $R_y(t)$ along the $x$ and $y$ directions, respectively.

## III. RESULTS

As mentioned earlier, we have considered both critical and off-critical fluid mixtures in our simulations. For the

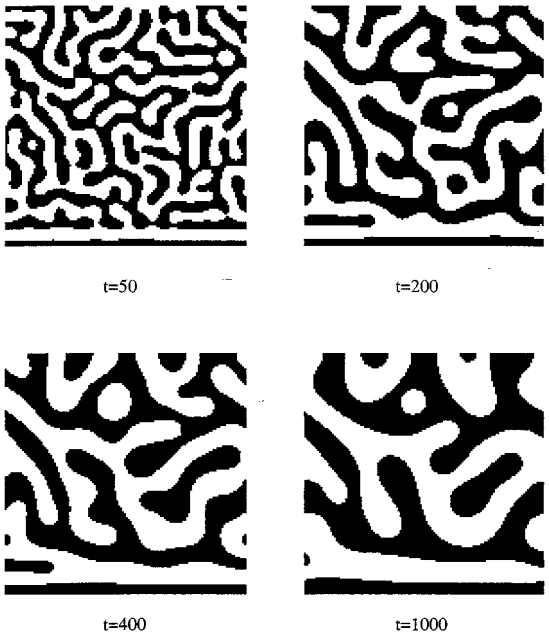


FIG. 1. ''Snapshots'' of order parameter for a typical run for $g=0$ (diffusion only case) with $x_0=0.5$. The preferentially attractive surface is located at the bottom. Note that the $A$-wetting layer and the $A$-depletion layer next to it are present throughout the course of the simulation.

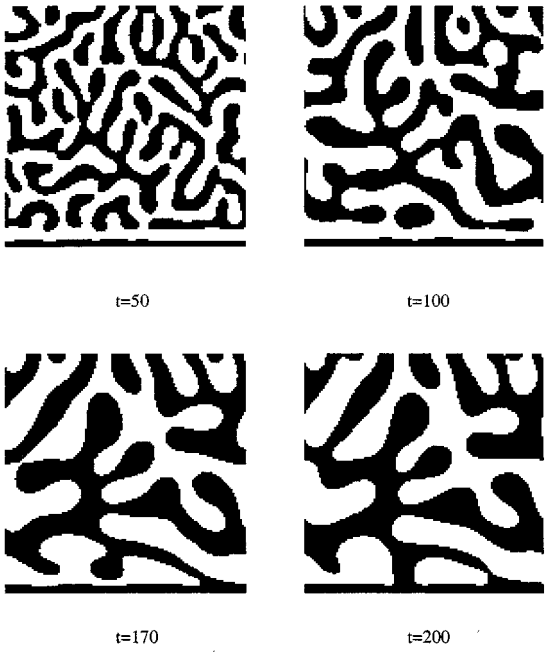


FIG. 2. ''Snapshots'' of order parameter for a typical run in the presence of hydrodynamics ($g=1$) with $x_0=0.5$. Note that the bulk domains now grow faster than in Fig. 1. At early times, $A$-wetting layer and -depletion layers are present, but at late times ($t>150$), the $A$ phase in the bulk connects itself to the wetting layer by rupturing the $A$-depletion layer.

critical mixture $x_0=0.5$, while for off-critical mixtures, we have chosen $x_0=0.3$, 0.7, and 0.8. Hydrodynamic effects can be neglected or included in the simulation by simply choosing the coupling parameter to be $g=0$ or 1. The exponent $p$ in the long-ranged surface interaction term [Eq. (11)] is chosen to be $p=1$ and $p=2$ [13,15]. Most of the results presented here are for $p=1$; for $p=2$ the results are similar to the $p=1$ case, for the deep quenches considered here. For the rescaled model [Eqs. (7)–(9)] considered here with $g=1$ and $\eta=1$, scaling arguments suggest that the late-time behavior of the two-dimensional system in the absence of any surface interactions, should be controlled by fluid inertia [13,21,22]. Thus, one would expect that the *bulk* domain-growth exponent should be $n\approx\frac{2}{3}$ at late times for a critical quench.

### A. Critical fluid mixture

Figures 1 and 2 show typical ''snapshots'' of the system, i.e., the order parameter distribution, at various times. Figure 1 shows ''snapshots'' of the diffusive case ($g=0$), and Fig. 2 shows the corresponding domain morphology in the presence of hydrodynamics ($g=1$). The preferentially attracting surface is located at the bottom ($y=0$), and the wetting layer develops near this surface. The wetting phase (component $A$ in our notation) is denoted by black and the other phase is left blank. Let us first describe the domain formation in the diffusive case (Fig. 1). We find that the $A$-rich wetting layer forms very quickly on the surface, which is followed by a $B$-rich layer. This alternating layer formation takes place only near the surface, and a more familiar interconnected morphology of the domains is seen as one further proceeds into the bulk. The wetting layer thickness as well as the bulk domain size increases with time. Note the presence of an alternating $A$-rich and $B$-rich layer (or equivalently an $A$-depletion layer) near the surface throughout the course of the simulation. This surface-directed structure formation was first theoretically formulated by Ball and Essery [12] and was observed in various simulations [7,13–16] and in experimental [8–11] studies. The corresponding density profile for the $A$ component shows a damped oscillatory form as a function of distance from the surface. This has also been observed and characterized in detail in many previous studies.

In the presence of hydrodynamic interactions, the bulk domains can be clearly seen to grow faster than the purely diffusive case when one compares Fig. 1 with Fig. 2 (for example, at $t=200$). At early times ($t\leqslant 100$), there is a well-defined wetting layer and a depletion layer near the surface, as in the case of purely diffusive growth. Over this time regime, the wetting layer thickens diffusively. Subsequently, hydrodynamics affect domain formation in the following way. At around $t\approx 150$, the $A$ phase in the bulk flows toward the surface and *breaks* the $A$-depletion layer. The wetting-layer and $A$ phase in the bulk thus get connected at this stage. As we discuss shortly, this manifests into a larger exponent for the wetting layer growth with time. The perforation of the $A$-depletion layer takes place only in the presence of hydrodynamic interactions. Such a rupture of the depletion layer has indeed been observed in experiments with thin polymer films [30,31], and suggested [30] as the mechanism behind the transient surface roughening of these thin films [32].

Before we carry out a more quantitative analysis for the wetting layer growth in the presence of hydrodynamics, let us first discuss the behavior of bulk domains in the presence of hydrodynamics. In Fig. 3 we show a log-log plot of the

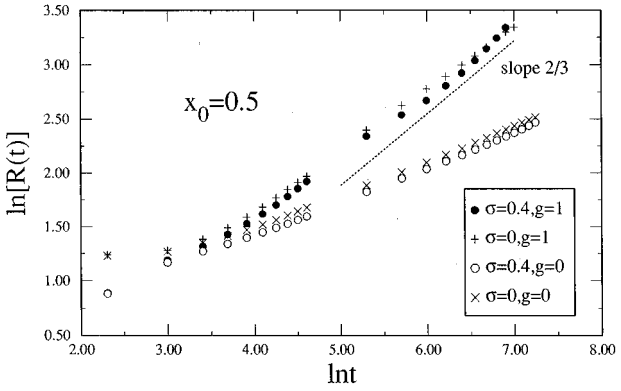


FIG. 3. Characteristic bulk domain size $R(t)$ for critical quench plotted vs time $t$ in a log-log scale for both diffusive ($g=0$) and hydrodynamic cases ($g=1$), both in the absence ($\sigma=0$) and presence ($\sigma=0.4$) of surface interactions. For diffusive cases the growth exponent is given by $n\approx 0.3$, and for hydrodynamic cases $n\approx 0.6$. A line of slope $\frac{2}{3}$ is shown as a guide to the eye.

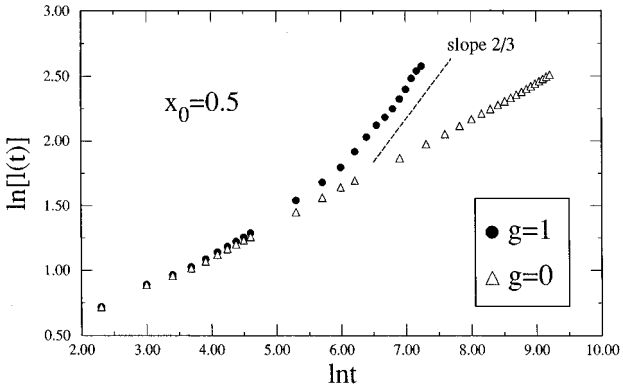


FIG. 4. Wetting layer thickness for critical quench $l(t)$ plotted vs time $t$ in a log-log scale for $g=1$ and $g=0$. For $g=0$, the growth exponent for the wetting layer $\theta\approx 0.3$ throughout the course of the simulation. For $g=1$, $\theta$ has a diffusive value of $\approx 0.3$ at early times, but at late times it becomes comparable with that of the bulk domain growth exponent ($\theta\approx 0.6$). A line of slope $\frac{2}{3}$ is shown as a guide to the eye.

average domain size $R(t)$ vs time $t$ both in the presence ($g=1$) and absence of hydrodynamics ($g=0$). For both $g=1$ and $g=0$, we study two cases, each having the presence of a symmetry-breaking surface, but in one case the surface interaction is turned off ($\sigma=0$). For $\sigma=0$, we find that the average domain size in $x$ and $y$ directions fall basically on top of each other. In this case, we compute $R(t)$ by taking averages of $R_x(t)$ and $R_y(t)$. In the presence of the surface interaction ($\sigma=0.4$), bulk domain sizes are computed over a subregion of the whole system with the same $L_x$ but starting at a layer 20 lattice sites away from the wetting surface in the $y$ direction. Even then, we find that the calculation of $R_x(t)$ is influenced by the growing wetting layer. $R_y(t)$ was unaffected, however, and is used as a measure of the bulk domain size in the presence of surface interactions [$R(t)$ [$\mathrm{R(t)}\equiv R_y(t)$]. As can be seen in Fig. 3 this measure of bulk domain size fall on top of the one in the absence of surface interactions, both in the presence and absence of hydrodynamics. Results shown in Fig. 3 are averaged over 30 runs for $g=1$, $\sigma=0.4$; 14 runs for $g=1$, $\sigma=0.0$; and 10 runs in each case of purely diffusive growth ($g=0$). When $g=0$, the value of the bulk domain growth exponent is found to be $n\approx 0.3$ for both $\sigma=0$ and 0.4. As expected, bulk domain growth is accelerated in the presence of hydrodynamics for ($t\geqslant 50$), and the growth exponent is now given by $n\approx 0.6$ for both $\sigma=0$, and 0.4. This value of $n$ is roughly consistent with theoretical prediction of $n=\frac{2}{3}$ for a two-dimensional fluid mixture in the inertial regime. The value of $n$ is also similar to those found in previous simulations where the authors did not enforce the incompressibility condition [20–22] on the fluid ($\vec{\nabla}\cdot\vec{v}=0$).

We now turn to analyzing growth of the wetting layer. Figure 4 shows a log-log plot of the wetting layer thickness $l(t)$ vs time $t$ for $g=1$ along with the corresponding layer thickness in the absence of hydrodynamics. At early times ($t<150$), the thickness of the wetting layer for $g=1$ falls right on top of the one computed for the purely diffusive case. The exponent for the wetting layer growth over this early time regime is found to be $\theta\approx 0.3$, exactly the same as the one for $g=0$ case. At late times, the exponent for the wetting layer growth in the presence of hydrodynamics ($\theta\approx 0.6$) is roughly consistent with the inertia-dominated *bulk* growth exponent.

It is clear from Fig. 4 that hydrodynamics does not influence wetting layer growth before $t<150$. Comparing with Fig. 3 we observe that the bulk domain growth is influenced by hydrodynamics at somewhat earlier times ($t\approx 50$) for the parameter values chosen here. Why the effect of hydrodynamics sets in at a later time on the wetting layer growth, than on domains growing in the bulk? This is due to the presence of the solid wetting wall where the fluid velocity is zero at all times. At earlier times, the fluid velocity near the wall is smaller than in the bulk and the wetting layer remains thin. Subsequently, at around $t=150$, the wetting component in the bulk flows through the depletion layer and connects to the wetting layer at the surface. The growth exponent begins to increase at this stage from the diffusive value of about 0.3 and crosses over to the hydrodynamic exponent. Eventually, when $t>500$, $n$ becomes comparable to the growth exponent of the bulk domains. We should point out that Marko [7] has conjectured this late onset of hydrodynamics for wetting layer growth, and the flow of the wetting component to the wall as the mechanism behind the faster growth of the wetting layer under the influence of hydrodynamics. The perforation of the depletion layer and the connection of the wetting layer to the bulk fluids have also been observed in recent experiments [30].

The shape of the density profile function $n(y,t)$ for $g=1$ at early times, is similar to that observed in Ref. [13] in the absence of hydrodynamics. The density profile shows damped oscillations as one moves away from the surface along the $y$ direction, with the oscillations dying out as the bulk system is approached. As time passes after the quench, the characteristic wavelength of the oscillations becomes larger, indicating the growth of the underlying wetting layer. We test the dynamical scaling hypothesis for the density profile by plotting $n(y,t)$ vs $y/l(t)$ in Figs. 5(a) and 5(b), for early and late times, respectively. We can see from these figures that scaling for the density profile is reasonably satisfied in each case, but the shape of the scaling function at

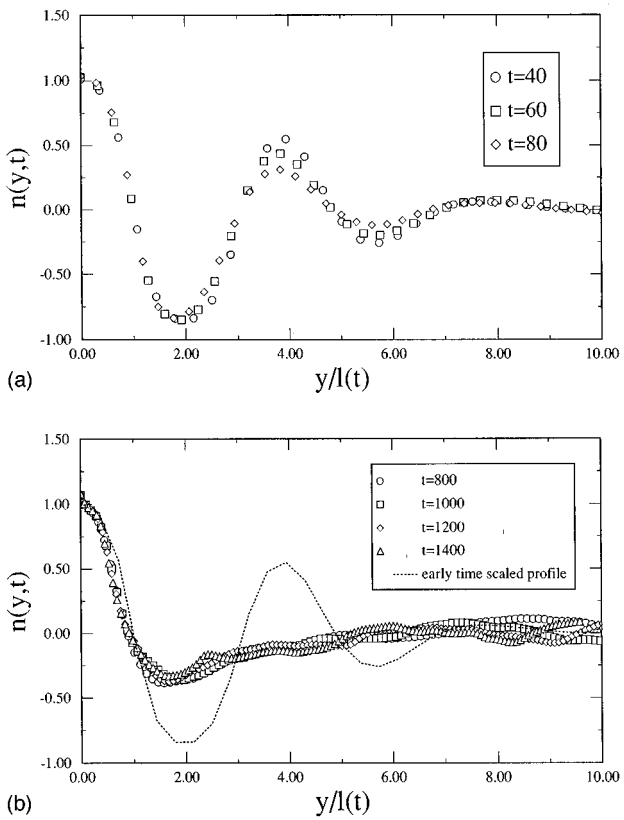


FIG. 5. (a) Test of dynamical scaling for the density profile of the wetting layer for critical quench with $g=1$. Scaling holds reasonably well for distance near the surface, and at these early times, the scaling function is similar to the purely diffusive case [13]. (b) Same as (a) at late times. Again scaling holds reasonably well for distance near the surface, but the scaled profile is shallower than that for early times.

late times is different from the corresponding one at earlier times. One can clearly observe in Fig. 5(b) that the density profile becomes shallower in the late stages because of the invasion of the $A$ component in the bulk into the $A$-depletion layer. Our results suggest that although there are two distinct mechanisms for wetting layer growth—diffusive and hydrodynamic—the wetting layer thickness $l(t)$ is the dominant length scale near the wetting surface throughout the growth of the layer.

### B. Off-critical fluid mixtures

#### *1. Majority component wets the substrate*

In this case, we have studied two different concentrations for the wetting component: $x_0=0.7$ and $x_0=0.8$. Figure 6 shows ''snapshots'' for a typical run for $x_0=0.7$ and $g=1$. It is interesting to note that at early times, the minority phase forms a layer next to the wetting layer formed by the majority component, although the morphology of the bulk minority phase is quite different. This feature of surface-induced phase separation has been observed in previous simulations for the purely diffusive case [33]. The flat layer of the minority phase remains intact in the purely diffusive case almost indefinitely. However, in the presence of hydrodynamic interactions, this $A$-depletion layer breaks into droplets and

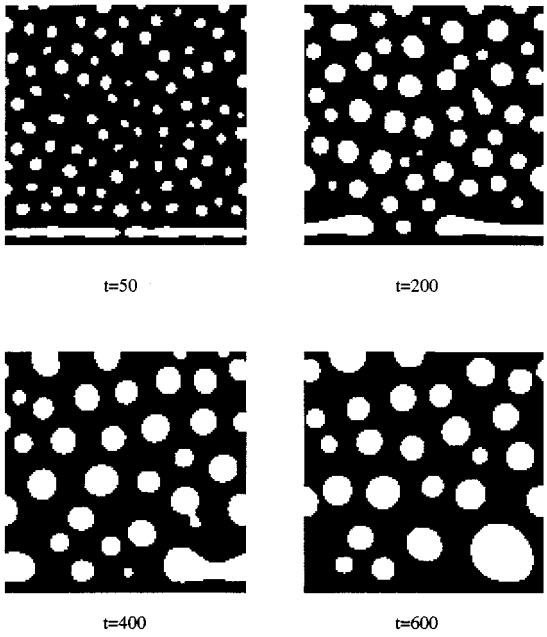


FIG. 6. ''Snapshots'' of order parameter for a typical run with $g=1$ and $x_0=0.7$. The minority phase forms droplets in the bulk, but forms a flat layer at early times, right above the wetting layer. At late times, the wetting phase in the bulk flows to the surface and breaks this layer.

the $A$-wetting layer gets connected to the bulk majority phase. Similar to the critical mixture, this is when the growth exponent for the wetting layer starts increasing from the diffusive value of $\frac{1}{3}$ and crosses over to a value of $\frac{2}{3}$ (Fig. 7). The density profile for $x_0=0.7$ shows a similar behavior to the critical mixture case: good scaling for the density profiles is found once the purely diffusive regime and the hydrodynamic regime are separated out as in Figs. 5(a) and 5(b). Again, the scaling function at late times does show a shallower minimum due to the invasion of the majority phase through the depletion layer and the corresponding rupture of it.

The situation is somewhat different for $x_0=0.8$. For this volume fraction the mixture is almost on the mean-field spin-

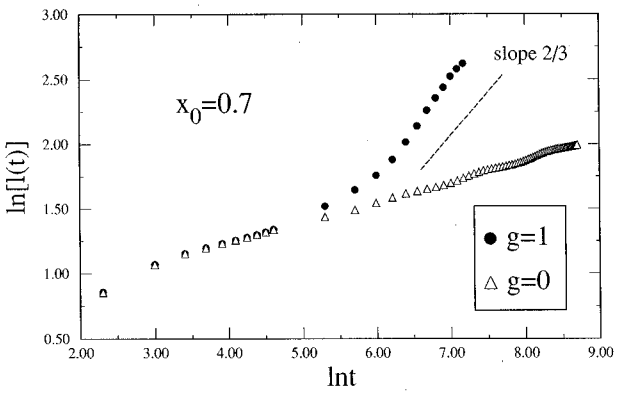


FIG. 7. Wetting layer thickness $l(t)$ plotted vs time $t$ in a log-log scale for $x_0=0.7$. For $g=0$, the growth exponent for the wetting layer $\theta\approx0.3$ throughout the course of the simulation. For $g=1$, $\theta$ has a diffusive value of $\approx0.3$ at early times. But at late times $\theta\approx0.6$. A line of slope $\frac{2}{3}$ is shown as a guide to the eye.

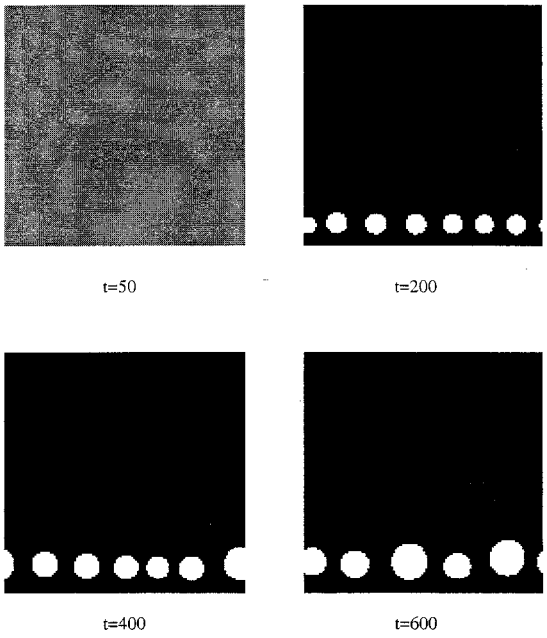


FIG. 8. ''Snapshots'' of order parameter for a typical run for $g=1$ and $x_0=0.8$. Note that the minority phase forms droplets only near the wetting surface.

odal line and in the absence of thermal fluctuations (as in our case) nucleation of minority domains takes place solely from the fluctuations in the initial value of the order parameter. If the spread in the initial values of the order parameter is not large, bulk minority domains may nucleate after a long waiting period. However, near the wetting surface, the majority phase is sucked into the surface quickly, and locally the barriers to form minority droplets are reduced. Thus, minority droplets first form near the surface right above the majority wetting layer, before any such droplets start appearing in the bulk. This is clearly demonstrated in Fig. 8 at the early time snapshots for the order parameter.

In the absence of hydrodynamics, wetting-layer growth for $x_0=0.8$ has been studied by Brown, Chakrabarti, and Marko [33]. They have found that the wetting layer thickness initially grows as $t^{1/3}$, but once minority droplets nucleate and start growing, $l(t)$ roughly follows a *slower* power law, $l\sim t^{1/6}$, possibly due to the *screening* effect of the droplet layer. This is shown in Fig. 9 for $g=0$. On the contrary, this slowdown of wetting-layer growth is not observed in Fig. 9 in the presence of hydrodynamic interactions ($g=1$). In this case, although the $A$ phase in the bulk and wetting layer are well connected, flow of the majority component through the minority droplets is difficult. As a result, we see a diffusion-dominated growth behavior for the wetting layer: $\theta\approx 0.33$ throughout the course of the simulation.

### *2. Minority component wets the substrate*

Snapshots for the evolution of the system for $x_0=0.3$ are shown in Fig. 10 for $g=1$. Next to the interacting wall we find a wetting layer composed of the minority phase, and another layer rich in the majority component immediately following the wetting layer. Farther from the wall are circu-

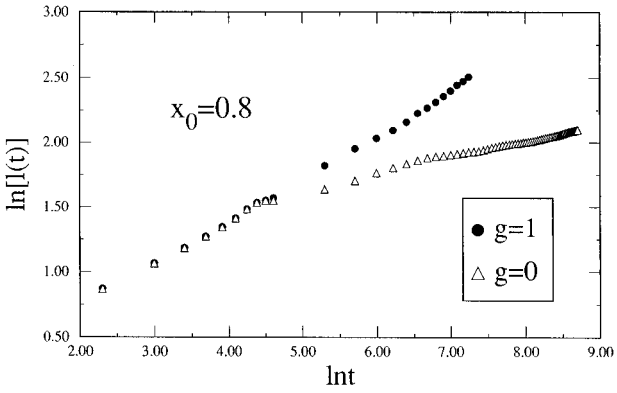


FIG. 9. Wetting-layer thickness $l(t)$ plotted vs time $t$ in a log-log scale for $x_0=0.8$. For $g=0$, the growth exponent for the wetting layer is approximately 0.3 at early times, but crosses over to a slower exponent of 0.16 at late times, possibly due to the ''screening'' effect of the minority droplets nucleating above the wetting layer at the wall [33]. For $g=1$, $\theta$ is approximately equal to 0.3 at all times.

lar domains rich in the minority component. For this composition, the quench takes place in the unstable part of the phase diagram and the bulk minority domains nucleate and grow spontaneously. Although the bulk pattern for the minority phase is circular droplets, note that the pattern is aligned with the interacting wall. The different pattern created near the wall is a result of mass transport caused by the creation of the wetting layer at early times. We show the growth of the wetting layer in Fig. 11 in a log-log plot. For $x_0=0.3$, since the wetting component in the bulk never flows to the surface, the thickening of the wetting layer is controlled by the diffusive mechanism. Thus the growth exponent for the wetting layer is comparable to that of the same mixture with $g=0$ [34].

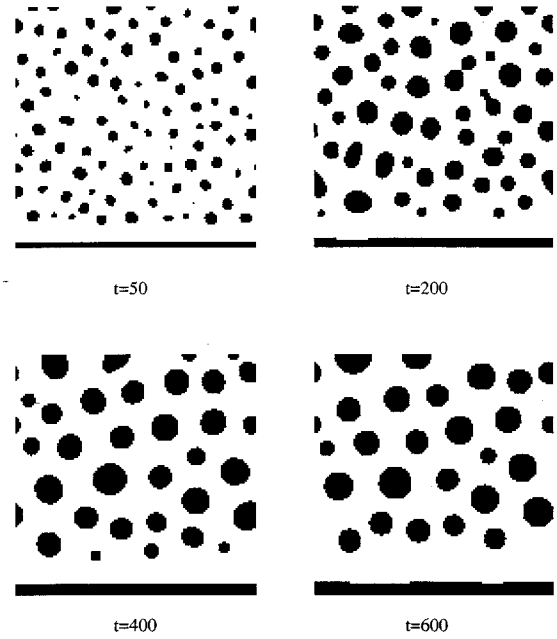


FIG. 10. ''Snapshots'' of order parameter for a typical run for $g=1$ and $x_0=0.3$.

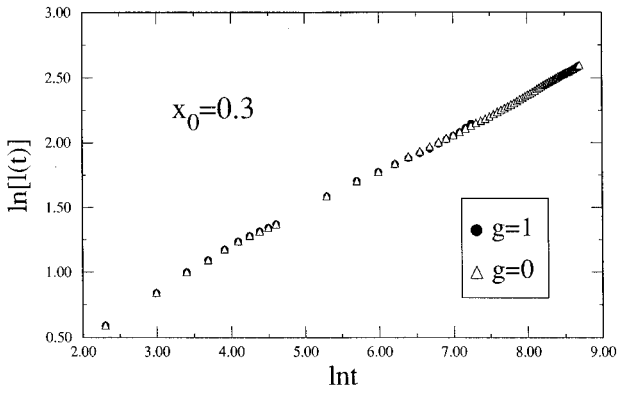


FIG. 11. Wetting-layer thickness $l(t)$ plotted vs time $t$ in a log-log scale for $x_0=0.3$. For $g=0$, the growth exponent for the wetting layer is approximately 0.3 at all times. For $g=1$, $\theta$ has the same value here as in the purely diffusive case.

## IV. SUMMARY AND CONCLUSIONS

We have numerically studied effects of hydrodynamic interactions on wetting layer growth in a binary fluid mixture undergoing spinodal decomposition. Our model calculations are carried out for two-dimensional incompressible binary fluid mixtures of either critical or off-critical concentrations, in the presence of a preferentially attractive surface. We have computed the bulk domain size, the wetting layer thickness, and the density profile function. For critical concentration, we have found that the growth of bulk domain size is characterized by an exponent $n\approx 0.6$, which is roughly consistent with the scaling result in two dimensions when inertial effects of the fluid mixture dominate. The wetting layer (for the preferentially attracted $A$ component) grows diffusively at early times with an exponent $\theta\approx 0.3$. In this time regime, the structure of the phase-separated fluid near the wall consists of an alternating $A$-rich and $B$-rich layer (or equivalently an $A$-depletion layer). A larger growth exponent for the wetting layer, comparable with the bulk domain growth exponent, is found at late times. This crossover from diffusive growth occurs when the wetting component in the bulk ($A$ phase) flows through the previous $A$-depletion layer and connects to the wetting layer at the surface. The density profile shows characteristic oscillations near the surface with oscillations dying out as one moves away from the surface into the bulk system. The density profile becomes shallower when the $A$ phase in the bulk invades into the surface area. The dynamical scaling hypothesis for the density profile function works reasonably well near the wetting surface, suggesting that the wetting layer thickness is the dominant length scale near the surface.

For off-critical concentrations, the hydrodynamic effect on the growth of the wetting layer is found to depend on the concentration of the wetting component. When the wetting component is the majority phase, flow of the $A$ component from the bulk to the wall is possible rupturing the $A$-depletion layer next to the wetting layer. This, again, leads to a larger growth exponent for the wetting layer. However, when the wetting component is a minority component of the mixture, such a flow of the wetting component from the bulk to the wall is not seen in the simulations. For this reason, the wetting-layer growth exponent is similar to the diffusive case for such an off-critical composition.

Results from this two-dimensional simulation may not be directly applicable for a detailed understanding of experimental results of wetting-layer growth. However, this simulation has provided some insight into the role played by hydrodynamics on the wetting-layer growth for various concentrations of the fluid mixture. For example, our results for the critical composition support a recent scaling analysis by Marko, who has suggested that the growth of the wetting layer is characterized by the same growth exponent as the bulk domains. This simulation also confirms Marko's conjecture that the effect of hydrodynamics on wetting-layer growth will take place at a later time than its effect on bulk domains due to the no-slip boundary condition on the fluid velocity at the wall. More importantly, our simulations provide strong evidence that the flow of the wetting component to the wall under the influence of hydrodynamics is the mechanism behind the faster growth of the wetting layer. The rupture of the depletion layer and the connection of the wetting layer to the bulk fluids have also been observed in recent experiments.

## ACKNOWLEDGMENTS

Acknowledgment is made to the Donors of the Petroleum Research Fund, administered by the American Chemical Society for partial support of this work. This work has also been supported by the Graduate School of Kansas State University. We thank Professor R. Fox, Professor J. Marko, and Professor J. Vinals for stimulating discussions. Computations have been carried out in the Convex-Exemplar machines at Kansas State University and in the National Center for Supercomputing Applications, Urbana-Champaign. This work has also been supported by National Science Foundation Grant No. DMR-9413513.

[1] P. C. Hohenberg and B. I. Halperin, Rev. Mod. Phys. **49**, 435 (1977).

[2] J. D. Gunton, M. Miguel, and P. S. Sahni, in *Phase Transition and Critical Phenomena*, edited by C. Domb and J. L. Lebowitz (Academic, New York, 1983), Vol. 8.

[3] I. M. Lifshitz and V. V. Slyozov, J. Phys. Chem. Solids **19**, 35 (1961).

[4] E. D. Siggia, Phys. Rev. A **20**, 595 (1979).

[5] H. Furukawa, Physica A **204**, 237 (1994).

[6] A. J. Bray, Adv. Phys. **43**, 357 (1994).

[7] J. F. Marko, Phys. Rev. E **48**, 2861 (1993).

[8] R. A. L. Jones, L. J. Norton, E. J. Kramer, F. S. Bates, and P. Wiltzius, Phys. Rev. Lett. **66**, 1326 (1991).

[9] G. Krausch, C. Dai, E. J. Kramer, and F. S. Bates, Phys. Rev. Lett. **71**, 3669 (1993).

[10] G. Krausch, C. A. Dai, E. J. Kramer, J. F. Marko, and F. S.

Bates, Macromolecules **26**, 5566 (1993).
[11] G. Krausch, E. J. Kramer, F. S. Bates, J. F. Marko, G. Brown, and A. Chakrabarti, Macromolecules **27**, 6768 (1994).
[12] R. C. Ball and R. L. H. Essery, J. Phys. Condens. Matter **2**, 10303 (1990).
[13] G. Brown and A. Chakrabarti, Phys. Rev. A **46**, 4829 (1992).
[14] S. Puri and K. Binder, Phys. Rev. A **46**, R4487 (1992).
[15] Z. Jiang and C. Ebner, Phys. Rev. B **39**, 2501 (1989).
[16] P. Keblinski, W.-J. Ma, A. Maritan, J. Koplik, and J. R. Banavar, Phys. Rev. E **47**, R2265 (1993); W.-J. Ma, P. Keblinski, A. Maritan, J. Koplik, and J. R. Banavar, *ibid*. **48**, R2362 (1993).
[17] P. Wiltzius and A. Cumming, Phys. Rev. Lett. **66**, 3000 (1991); B. Q. Shi, C. Harrison, and A. Cumming, *ibid*. **70**, 206 (1993).
[18] S. M. Troian, Phys. Rev. Lett. **71**, 1399 (1993); see, however, P. Keblinski, W.-J. Ma, A. Maritan, J. Koplik, and J. R. Banavar, *ibid*. **72**, 3738 (1994); S. M. Troian, *ibid*. **72**, 3739 (1994).
[19] M. S. Miguel, M. Grant, and J. D. Gunton, Phys. Rev. A **31**, 1001 (1985).
[20] J. E. Farrel and O. T. Valls, Phys. Rev. B **40**, 7027 (1989).
[21] T. Lookman, Y. Wu, F. J. Alexander, and S. Chen, Phys. Rev. E **53**, 5513 (1996).
[22] Y. Wu, F. J. Alexander, T. Lookman, and S. Chen, Phys. Rev. Lett. **74**, 3852 (1995).
[23] O. T. Valls and J. E. Farrel, Phys. Rev. E **47**, R36 (1989).
[24] D. Jasnow and J. Vinals, Phys. Fluids **8**, 660 (1996).
[25] M. Gurtin, D. Polignone, and J. Vinals, Math. Methods Appl. Sci. **6**, 815 (1996).
[26] C. A. J. Fletcher, *Computational Techniques for Fluid Dynamics* (Springer-Verlag, Berlin, 1988), Vol. 2.
[27] K. Aziz and J. D. Hellums, Phys. Fluids **10**, 314 (1967).
[28] In general, one may also have a pressure term $-\nabla p$ on the right-hand side of Eq. (7). In the vorticity-stream function formulation the pressure term in the modified Navier-Stokes (NS) equation [Eq. (7)] disappears because one considers a curl of the modified NS equation. This has been discussed in Refs. [24,25]. We would also like to note that sound modes play only a minor role in spinodal decomposition as in the case of critical dynamics. This has been discussed by J. E. Farrell and O. T. Valls, Phys. Rev. B **42**, 2353 (1990).
[29] W. H. Press, S. A. Teukolsky, W. T. Vettrling, and B. P. Flannery, *Numerical Recipes in Fortran*, 2nd ed. (Cambridge University Press, New York, 1992).
[30] J. Heier, K. D. Jandt, E. J. Kramer, and F. S. Bates, Bull. Am. Phys. Soc. **41**, 51 (1996); K. D. Jandt, J. Heier, F. S. Bates, and E. J. Kramer, Langmuir **12**, 3716 (1996).
[31] T. Slawecki *et al.* (unpublished); see also T. Slawecki, Ph.D. thesis, Pennsylvania State University (1996).
[32] A somewhat different explanation for the transient surface roughening seen in experiments with a free-surface has been proposed by P. Keblinski, S. K. Kumar, A. Maritan, J. Koplik, and J. R. Banavar, Phys. Rev. Lett. **76**, 1106 (1996).
[33] G. Brown, A. Chakrabarti, and J. F. Marko, Phys. Rev. E **50**, 1674 (1994).
[34] The domain growth exponent in this regime is found to be $n \approx 0.4$ in the presence of hydrodynamics [22].